

Dispersion Relation Gaps and Neutrino Flavor Instabilities in Fast Modes

Lei Ma^{*} and Huaiyu Duan[†]

Authors' institution and/or address

*This line break forced with *

(Dated: August 7, 2017)

Abstract

ABSTRACT PLACEHOLDER

^{*} Also at Physics Department, XYZ University.

[†] Second.Author@institution.edu

I. INTRODUCTION

(Should talk about some very very basic backgrounds like the applications and why it is important.)

Neutrino flavor conversions in vacuum are linear effects in Schrodinger equation, in other words, the vacuum Hamiltonian doesn't depend on the state of neutrino flavors. However, neutrinos propagate in dense neutrino media demonstrate highly nonlinear flavor transformations due to forward scattering interactions of neutrinos. Such interactions lead to flavor conversions instabilities. The technique that is used to investigate the nonlinear neutrino flavor conversion is linear stability analysis [1, 2]. Recent studies by I. Izaguirre, G. Raffelt, and I. Tamborra show that linear stability analysis indicates the dispersion relation [3]. They also showed that dispersion relation can be defined and calculated in linear regime of neutrino flavor conversions. Moreover, they concluded that neutrino flavor conversion instabilities occur within gaps in dispersion relation. We argue that neutrino flavor conversion instabilities is not exactly mapped to gaps in dispersion relation for discrete emission with more than two angles or continuous angular distributions of neutrino emissions. To begin with, we review reference 3 to explain the dispersion relation in Sec. II.

II. DISPERSION RELATION OF NEUTRINO FLAVOR CONVERSION

We consider two-flavor scenario of neutrino oscillations. As an initial condition, all neutrinos and antineutrinos are emitted approximately as electron flavors. For the purpose of linear stability analysis, the single particle density matrix for neutrinos is explicitly defined as

$$\rho = \frac{1}{2} \begin{pmatrix} 1 & \epsilon \\ \epsilon^* & -1 \end{pmatrix}. \quad (1)$$

To determine the flavor evolution, Liouville equation of neutrinos is used,

$$i(\partial_t + \mathbf{v} \cdot \nabla)\rho = [H, \rho], \quad (2)$$

where H is the Hamiltonian for neutrino oscillations. Density matrix and equation of motion for antineutrinos are defined in the same maner with the corresponding Hamiltonian for antineutrinos.

In principle, neutrino oscillations Hamiltonian depends on three different contributions, vacuum oscillations H_v , interactions with matter H_m , and interactions with neutrinos themselves $H_{\nu\nu}$. The concentration of this work is on fast neutrino oscillations, which would occur even without neutrino mass differences. However, the vacuum term can always be combined with matter term by redefining new matter potential. Thus neglecting vacuum term doesn't change the formalism of linear stability analysis. For completeness, we write down the vacuum oscillations term

$$H_v = -\frac{\omega_v}{2}\sigma_3, \quad (3)$$

where $\omega = \frac{\delta m^2}{2}$ with δm^2 being the mass squared difference in this two flavor scenario. Interaction with matter is described by matter potential

$$H_m = \frac{1}{2}\lambda\sigma_3. \quad (4)$$

where $\lambda = \sqrt{2}G_F n_e$. G_F is the Fermi constant and n_e is the number density of electrons in the background.

In order to calculate the neutrino forward scattering, the spectrum of neutrino (antineutrinos) distributions $f_{\nu_e(\bar{\nu}_e)}(\hat{\mathbf{v}}, E)$ and $f_{\nu_x(\bar{\nu}_x)}(\hat{\mathbf{v}}, E)$ is required, where $\hat{\mathbf{v}}$ is the velocity direction of neutrinos (antineutrinos). Neutrino forward scattering potential is

$$H_{\nu\nu} = \sqrt{2}G_F \iint \frac{d\cos\theta' d\phi'}{4\pi} v^\mu v'_\mu \int \frac{E'^2 dE'}{2\pi^2} (\rho_n - \bar{\rho}_n), \quad (5)$$

where $v^\mu = (1, \sin\theta \cos\phi, \sin\theta \sin\phi, \cos\theta)^T$ is the four velocity of (anti)neutrinos in spherical coordinate system, ρ_n and $\bar{\rho}_n$ are the flavor density matrix of neutrino ensemble,

$$\rho_n(\hat{\mathbf{v}}, E) = (f_{\nu_e}(\hat{\mathbf{v}}, E) - f_{\nu_x}(\hat{\mathbf{v}}, E)) \rho \quad (6)$$

$$\bar{\rho}_n(\hat{\mathbf{v}}, E) = (f_{\bar{\nu}_e}(\hat{\mathbf{v}}, E) - f_{\bar{\nu}_x}(\hat{\mathbf{v}}, E)) \bar{\rho}. \quad (7)$$

In reference 3 the authors assumed that the distribution of ν_x and $\bar{\nu}_x$ are the same, namely $f_{\nu_x}(\hat{\mathbf{v}}, E) - f_{\bar{\nu}_x}(\hat{\mathbf{v}}, E) = 0$. We follow the same simplification in this paper. In addition, we following the same definition of electron lepton number (ELN) of neutrinos travelling in direction $\hat{\mathbf{v}}$,

$$G(\hat{\mathbf{v}}) = \sqrt{2}G_F \int \frac{E'^2 dE'}{2\pi^2} (f_{\nu_e}(\cos\theta', \phi', E') - f_{\bar{\nu}_e}(\cos\theta', \phi', E')). \quad (8)$$

The ELN is useful in linear stability analysis where we assumed that ϵ is small and evolve in the form $\epsilon_0 e^{-i(\Omega t - \mathbf{K} \cdot \mathbf{x})}$. In linear regime, constant matter background simply shifts the Fourier mode frequencies and doesn't generate or eliminate gaps in dispersion relation. Accordingly we neglect matter background.

Linear stability analysis of Eq. (2) for axial symmetric neutrino emission shows that

$$\det \left(\omega \mathbf{I} + \frac{1}{2} \begin{pmatrix} I_0 & 0 & 0 & -I_1 \\ 0 & -\frac{1}{2}(I_0 - I_2) & 0 & 0 \\ 0 & 0 & -\frac{1}{2}(I_0 - I_2) & 0 \\ I_1 & 0 & 0 & -I_2 \end{pmatrix} \right) = 0, \quad (9)$$

where

$$I_m = \int_{-1}^1 du G(u) \frac{u^m}{1 - (|k|/\omega) u}. \quad (10)$$

where we define $u = \cos \theta$. $|k|/\omega$ is defined as the refractive index of the wave n . For spectrum $G(u)$ without zero points, the forbidden region is given by $1 - (|k|/\omega) u \leq 0$. Two categories of solutions were found, namely the multi-azimuthal angle (MAA) solution and multi-zenith angle (MZA) solution [2]. The MAA solution is related to symmetry breaking in azimuthal angle only, which is determined by

$$\omega = \frac{1}{4}(I_0 - I_2). \quad (11)$$

The MZA solution is related to symmetry breaking in both azimuthal angle and zenith angle, which is

$$\omega = -\frac{1}{4} \left(I_0 - I_2 \pm \sqrt{(I_0 + I_2 - 2I_1)(I_0 + I_2 + 2I_1)} \right). \quad (12)$$

We denote the solution associated with + sign as MZA+, while the solution associated with - sign as MZA-. The two solutions are connected to each other in dispersion relations. In general, it doesn't provide physical insights to distinguish the two branches of solutions.

Eq. (9) is equivalent to dispersion relation defined in reference 3. In other words, the solutions (11) and (12) are dispersion relations $D(\omega, \mathbf{k})$ for a chosen direction of $\hat{\mathbf{k}} = \hat{\mathbf{z}}$.

HAVE TO EXPLAIN THE IDEA OF GAP AND INSTABILITY HERE.
Maybe Later?

III. INSTABILITIES AND GAPS

In reference 3, the authors relate gaps to instabilities of neutrino oscillations. The definition of dispersion relation gaps becomes clear in axial symmetric emission examples. We repeat the two zenith angles case discussed in reference 3 as a review.

We continue the discussion of axial symmetric neutrino emissions but with discretized zenith angles θ thus discretized u . In this case, the ELN is independent of azimuth angle ϕ . For neutrino emission with 2 zenith angles, the ELN spectrum can be written as

$$G(u) = \sum_{i=1}^2 g_i \delta(u - u_i). \quad (13)$$

The MAA solution becomes an equation of hypobola for ω and k , which has asymptotes $\omega = ku_i$ for $i = 1, 2$. Mathematically, the hyperbola equation has two solutions of $\omega(k)$ for any given real $k(\omega)$. The solutions are either real which indicates stable solutions or complex which indicates exponential growth in linear regime. On the other hand, non-existence of real solutions of $\omega(k)$ for given real $k(\omega)$ is equivalent to gap in dispersion relation. Thus the equivalence of gap and instabilities is guaranteed in neutrino emission with two-zenith-angle emission. Fig. 1 is a reproduction of Fig. 1 of reference 3. The dispersion relation is shown as black lines. To plot the complex ω , we define two quantities out of ω , the real part ω_R and $\omega_R \pm \omega_I$ as a combination of real part ω_R and imaginary part ω_I . The real part ω_R is shown as red solid lines and $\omega_R \pm \omega_I$ are shown as red dashed lines.

However, this conclusion can not be generalized to arbitrary number of emission angles. As an example, we perform linear stability analysis of the three zenith angles emission configuration which is determined by a cubic function both in ω and k . Thus three solutions of $k(\omega)$ for given real $\omega(k)$ are expected. As long as real solutions disappear, complex solutions emerge, which leads to instabilities occur even without an actual gap. As an example, we fix $\omega = 0.5$ for MAA solution (Fig. 1 lower left panel). The three solutions of k are $k = -4.6, 0.29, 1.2$. 0.2 which are all real and indicates no spatial instabilities. However, for another real $\omega = 0.2$, we find only one real solution $k = 0.4$ from dispersion relation. The other solutions are complex and proven to be $k = -0.557106 \pm 0.966535i$ where the value with positive imaginary part leads to exponential growth. This gap and instability inconsistency also exists in continuous angular distribution of neutrino emission.

In core collapse supernova, neutrino emission is not in discrete zenith angles. More

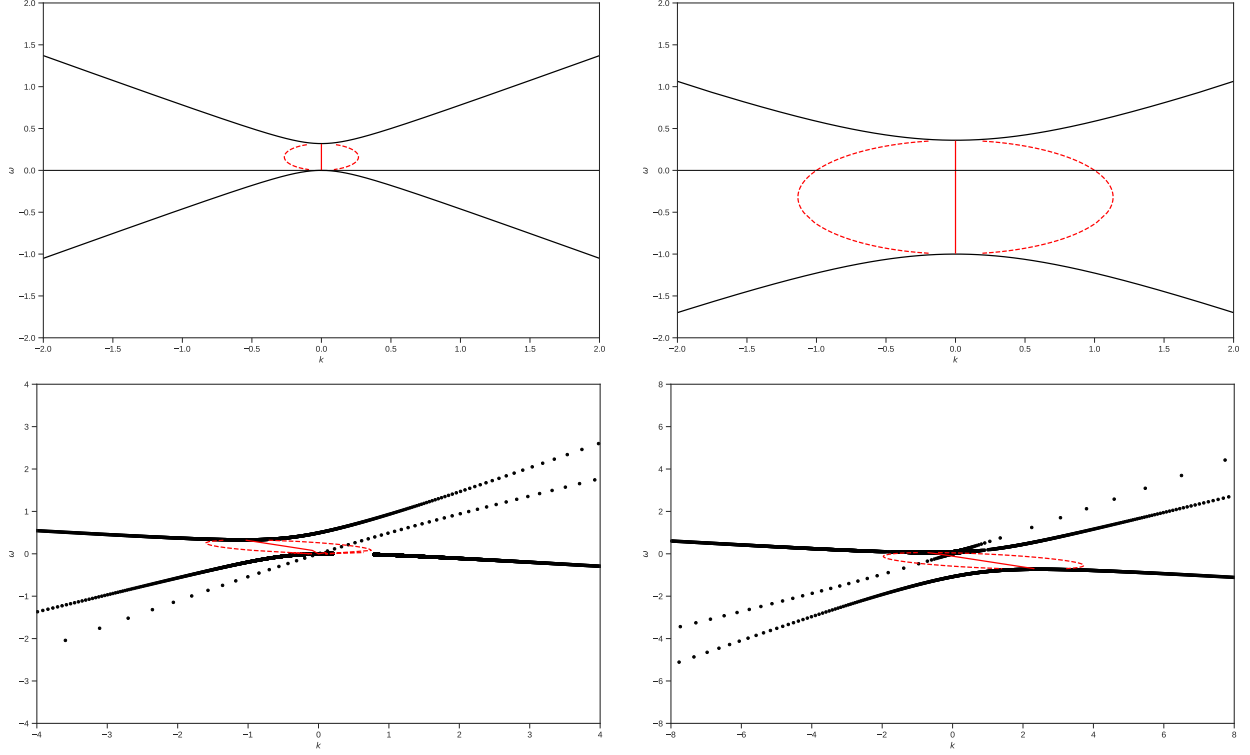


FIG. 1. Dispersion relation and instabilities of two zenith angles spectrum (upper panels) and three zenith angles spectrum (lower panels). The black lines are the dispersion relations and the colored dots are examples of complex ω for real k . The left panels shows the dispersion relation and linear stability analysis of MAA solutions. The mid and right panels show the dispersion relation of MZA solutions.

realistic models involves continuous zenith angle ELN spectra. In the earlier works of fast modes, Sawyer analyzed a box shaped angular distribution of neutrino emission [4]. To address the fact that instability does not always show up in dispersion relation as gap, we show that the relation between instability and gap in dispersion relation can break down for box spectrum with crossing.

We construct a box spectrum with value -0.1 within $u \in [-1, -0.3)$ and value 1 within $[-0.3, 1]$ as shown in the top left panel of Fig. 2. With the spectrum defined, we calculate the dispersion relation and find out complex values of k for real ω . The results show that both the MAA solution and MZA solutions contain only one curve. No gap is formed but we observe instabilities, which are plotted as colored dots.

The forbidden region is determined by the emission angles. But is the forbidden region worth mentioning here? I don't think so.

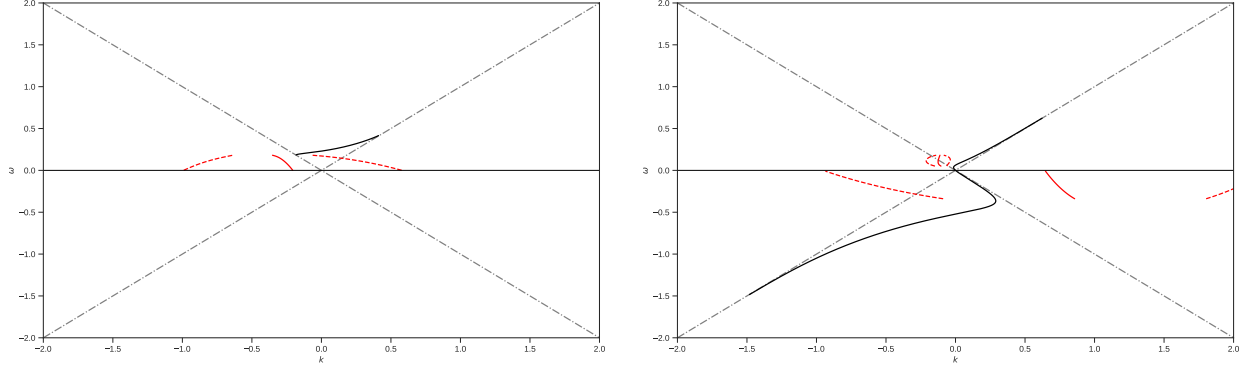


FIG. 2. Dispersion relation and linear stability analysis for box spectrum. The box spectrum is defined to be -0.1 within range $u \in [-1, -0.3)$ and 1 within range $u \in [-0.3, 1]$ as shown in the top left panel. The top right panel shows the dispersion relation and the complex k for real ω for MAA solution. The lower panels shows the dispersion relation and complex k for real ω for MZA solutions. Dashed gray lines are lines of $\omega = \pm k$ which sets the boundaries of the forbidden region for dispersion relation.

I could show the results for C4 since it has both MAA and MZA instabilities. But we care about complex k the most so I guess WC4 is fine.

Should I combine the MZA+ and MZA- solutions?

Font size in the plots are too small. But the font size depends on whether I need to combine MZA+ and MZA- solutions.

$\omega = 0$ lines in the plots should be made distinguishable from the DR.

IV. FROM GAP TO INSTABILITY

In the situations that the ELN spectrum has no crossing, gap indeed indicates instabilities, as shown in 3. In this section we prove that the instabilities in MAA, MZA+, or MZA- solution can only appear in either region $\omega \leq 0$ or region $\omega \geq 0$. As this suggests, the instability regions propagate only between the dispersion relation and the axis $\omega = 0$. We reproduce the calculation in 3 using the same Garching core-collapse supernova data set [5]. The spectrum shown in the left panel of Fig. 3 is polynomial fitting of the Garching 1D supernova simulation data.

I haven't put in the correct unit for omega and k yet!!!! Remake the plots with the correct unit

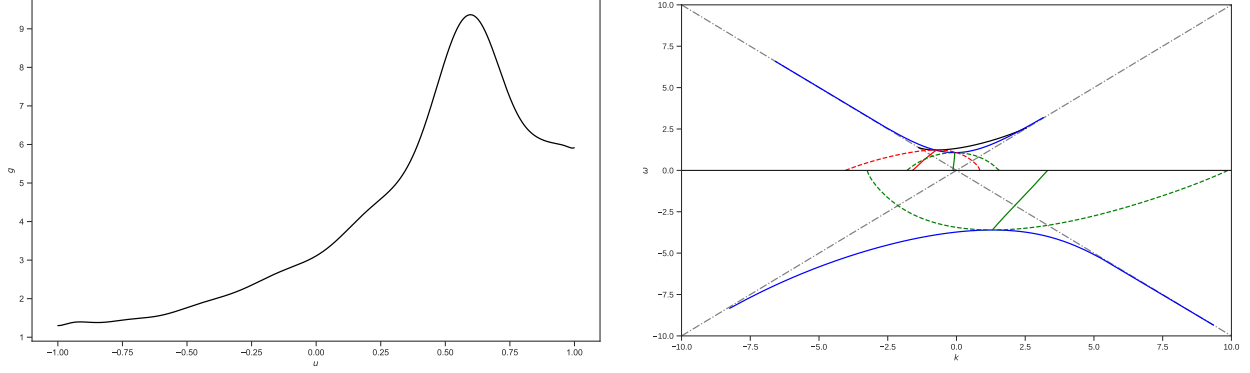


FIG. 3. Dispersion relation and linear stability analysis for a spectrum constructed from Garching 1D simulation data (left panel). From left to right, the sets of colored dots are the complex k for MAA solution, MZA-, and MZA+ solutions respectively.

For MAA solution of arbitrary spectrum, we write down the general form as

$$4 = \bar{I}_0 - \bar{I}_2, \quad (14)$$

where the I_m is defined in the preceeding sections. Explicitly, we have to solve the integral function to find out k for real ω ,

$$k = \frac{1}{4} \int G(u) \frac{1 - u^2}{\omega/k - u}. \quad (15)$$

For complex k , the integral can be decomposed into the principal value $\text{Re}(k)$ and imaginary part $\text{Im}(k)$ using Sokhotski–Plemelj theorem,

$$\text{Re}(k) = \frac{1}{4} \left(\mathcal{P} \int G(u) \frac{1 - u^2}{-u} \right) \quad (16)$$

$$\text{Im}(k) = \frac{\pi}{4} G(0) \text{Sign}(\omega) \text{Sign}(\text{Im}(k)). \quad (17)$$

We conclude from Eq. (17) that ω has to have the same sign as $G(0)$. What's more, the value of k at limit $\omega \rightarrow 0$ can be solved out of Eq. (16) and Eq. (17). For instabilities the imaginary part of k tells us the growth,

$$|\text{Im}(k)| = \frac{\pi}{4} |G(0)|. \quad (18)$$

Similar result is obtained for MZA solutions,

$$\left(4 \operatorname{Re}(k) - \mathcal{P} \int \frac{G(u)}{u} du + U_1\right)^2 - (\operatorname{Sign}(\omega \operatorname{Im}(k)) \pi G(0) + 4 \operatorname{Im}(k))^2 \quad (19)$$

$$= \left(\mathcal{P} \int \frac{G(u)}{u} du + U_1\right)^2 - 1 - 4U_0^2 \quad (20)$$

$$\left(4 \operatorname{Re}(k) - \mathcal{P} \int \frac{G(u)}{u} du + U_1\right) (\pi \operatorname{Sign}(\omega \operatorname{Im}(k)) G(0) + 4 \operatorname{Im}(k)) \quad (21)$$

$$= - \left(\mathcal{P} \int \frac{G(u)}{u} du + U_1\right) \pi \operatorname{Sign}(\omega \operatorname{Im}(k)) G(0), \quad (22)$$

where $U_m = \int G(u) u^m du$ and all the integrals are from -1 to 1 . The equations are quadratic in both $\operatorname{Re}(k)$ and $\operatorname{Im}(k)$ so the real solutions can be calculated and verified with linear stability analysis. The imaginary part $\operatorname{Im}(k)$

$$\operatorname{Im}(k) = -\frac{1}{4} \pi G(0) \operatorname{Sign}(\omega k_I) \left(1 + \frac{P \int \frac{G(u)}{u} du + \int G(u) u du}{4 \operatorname{Re}(k) - P \int \frac{G(u)}{u} du + \int G(u) u du}\right) \quad (23)$$

determines that the two solutions are either in the region $\omega > 0$ or in the region $\omega < 0$ which corresponds to MZA+ and MZA- solutions.

V. CONCLUSION

Appendix A: Plan of the paper

- Review fast mode oscillations
- State what has been done in Raffelt's paper.
- The conclusion is not true.
- Two zenith angles examples to prove that the number of solutions is the key.
- Three zenith angles examples to show that not exactly related to gap.
- Show that the continuous case is not related to gap at all. Box spectrum?
- Continuous spectrum or Garching group, data to show that we can prove the location of the instability.
- **Tweak the font size of plots.**

But I have a question. Is it really reliable? Should I use principal value integral for box spectrum DR?

We are still not crystal clear about the relation between gap and lsa .

-
- [1] A. Banerjee, A. Dighe, and G. Raffelt, Physical Review D **84**, 053013 (2011), arXiv:1107.2308 [hep-ph].
 - [2] G. Raffelt, S. Sarikas, and D. D. S. Seixas, Physical Review Letters **111**, 091101 (2013).
 - [3] I. Izaguirre, G. Raffelt, and I. Tamborra, Physical Review Letters **118**, 021101 (2017), arXiv:1610.01612.
 - [4] R. F. Sawyer, Physical Review Letters **116**, 1 (2016), arXiv:1509.03323.
 - [5] “The Garching Core-Collapse Supernova Archive, <http://wwwmpa.mpa-garching.mpg.de/ccsnarchive/archive.html>,”.